PHYSICAL REVIEW B VOLUME 25, NUMBER 12 15 JUNE 1982

Local-field effect in optical reflectance from adsorbed overlayers

Amitabha Bagchi
768 Huckleberry Way, Webster, New York 14580

Rubén G. Barrera
Institute of Physics, University of Mexico, Mexico 20, District Federal, Mexico

Ronald Fuchs
Ames Laboratory and Department of Physics, Iowa State University, Ames, Iowa 50011
(Received 16 February 1982)

The importance of the local-field effect in differential reflectance spectroscopy is demonstrated by means of numerical calculations done for the system of argon adsorbed on an aluminum substrate at two coverages. The calculations show that peaks in differential reflectance are not simply proportional to the adsorbate coverage, and their locations (in energy) change as the coverage is changed. Two models are considered for the substrate dielectric response—a local dielectric constant, and a nonlocal response based on the semiclassical infinite-barrier model. The local-field effect is shown to exist independent of the model considered for the substrate dielectric response. Connection is made with the available experimental data wherever appropriate.

I. INTRODUCTION

It was pointed out by Bagchi, Barrera, and Dasgupta[1] that the local-field effect might be important in the interpretation of certain aspects of the differential reflectance spectra obtained from weakly adsorbed species on a metal substrate. They focused attention on experiments[2,3] done with rare-gas atoms, chiefly argon adsorbed on aluminum, and showed that the local-field effect, i.e., the modification of the electromagnetic field at a given adsorbate atom because of the presence of other adsorbate atoms, could explain the observed movement of the optical-absorption peaks as the adsorbate coverage was changed. Their results were in qualitative agreement with the experimental data.

The treatment in Ref. 1 was brief and was based on a local screening model for the metal substrate. In this paper we present a more detailed account of the theory, and also consider the nonlocality of the dielectric response function of the background metal. We find that the main conclusions of Ref. 1 (hereafter referred to as I) hold even with the inclusion of nonlocal effects. This certainly buttresses the claim made in I about the importance of local-field effects in differential reflectance spectroscopy.

The physics of the problem under investigation can be discussed simply in the following terms. Consider an ordered two-dimensional array of adsorbed atoms located at $\{\vec{R}_{i,j}\}$ outside a metal surface, where the metal is assumed to occupy the region $z>0$. For a two-dimensional square array of lattice parameter a_l, the atomic locations are given by

$$\vec{R}_{i,j}=(ia_l, ja_l, -z_0)\ , \tag{1.1}$$

where $-\infty<i,j<\infty$, and z_0 denotes the separation between the adsorbate plane and the metal surface. When an electromagnetic wave is incident upon the system, each adsorbed atom feels an electric field which is the superposition of the external field (without adsorbates) and the dipolar field produced by all other atoms. This net field polarizes the atom, giving it a (time-varying) dipole moment $\vec{p}e^{-i\omega t}$, where

$$\vec{p}=\overleftrightarrow{\alpha}(\omega)\cdot(\vec{E}^{0}+\vec{E}_{\rm dip})\ , \tag{1.2}$$

$\overleftrightarrow{\alpha}(\omega)$ being the atomic polarizability tensor, and $\vec{E}^{0}$ and $\vec{E}_{\rm dip}$ the external and dipolar fields, respectively, at the location of the atom. We have assumed here that the incident light is monochromatic, having an angular frequency ω, and that its wavelength $\lambda=2\pi c/\omega$ is much greater than a_l so that the variation of $\vec{E}^{0}$ parallel to the surface can be ignored. The dipolar field at an adsorbate site can be decomposed into two terms,

$$\vec{E}_{\rm dip}=\vec{E}^{(1)}_{\rm dip}+\vec{E}^{(2)}_{\rm dip}\ , \tag{1.3}$$

where $\vec{E}_{dip}^{(1)}$ is the contribution to the dipolar field arising from dipoles in the adsorbate plane, and $\vec{E}_{dip}^{(2)}$ denotes the contribution to the field from image dipoles induced in the metal. Both these fields, in turn, depend on the dipole moment $\vec{p}$. If $\vec{E}_{dip}$ can be expressed in terms of $\vec{p}$, Eq. (1.2) may be solved for $\vec{p}$ as a function of the external field $\vec{E}^0$, thereby permitting us to define a dielectric response tensor $\overleftrightarrow{\epsilon}_a$ for the adsorbed layer. The differential reflectance from such a system can then be computed with the aid of microscopic formulas that were derived preciously,[4] and the result compared with experiments.

The dipolar field at an atomic site, say the one specified by $(0,0,-z_0)$, from all other dipoles in the adsorbate plane is given by[5]

$$\vec{E}_{dip}^{(1)} = \sum_{i,j=-\infty}^{\infty}{}' \frac{3[\vec{p}\cdot(\vec{R}_{ij}-\vec{R}_{00})](\vec{R}_{ij}-\vec{R}_{00})-\vec{p}(\vec{R}_{ij}-\vec{R}_{00})^2}{(\vec{R}_{ij}-\vec{R}_{00})^5}, \tag{1.4}$$

$$=\hat{z}(p_z/a_l^3)\xi_0-[\hat{x}(p_x/a_l^3)+\hat{y}(p_y/a_l^3)](\xi_0/2), \tag{1.5a}$$

where ξ_0 denotes the well-known two-dimensional sum evaluated by Topping,[6]

$$\xi_0=-\sum_{i,j=-\infty}^{\infty}{}' (i^2+j^2)^{-3/2}$$

$$=-9.0336.... \tag{1.5b}$$

The prime in all these sums indicates that the term with $i=j=0$ must be omitted. It is far more difficult, though, to evaluate the image field $\vec{E}_{dip}^{(2)}$. This was done in I within the local screening approximation and ignoring retardation effects. That procedure is discussed in some detail in this paper. We also try here to go beyond the local screening approximation by utilizing the results of recent studies[7–9] done by several authors on the theory of the dynamical screening of a dipole by a metal surface. In this paper we shall present results based on the semiclassical infinite-barrier (SCIB) model,[9] which has distinct advantages over the other models discussed in the literature.[7,8] The formalism developed by Feibelman[7] uses a random-phase approximation (RPA) jellium description of the metal, and calculates the induced field correctly only if the dipole is far from the metal surface. This is a severe limitation, and excludes some of the more interesting effects of nonlocality, e.g., the dispersion of the surface- and bulk-plasmon modes, and the electron–hole-pair excitation for large momentum transfer $\vec{Q}$ parallel to the surface. The work of Metiu and collaborators[8] is not particularly well suited to study the screening of an ordered overlayer of oscillating dipoles. The SCIB model, on the other hand, while not treating the diffuse nature of the metal surface correctly, includes the most important effects of nonlocality; it can be solved easily for arbitrary distance of the dipole from the surface and for different metals and it yields physically comprehensible results. That is why we use this model in our calculation.

Since the actual problem is fairly complicated, we shall make certain simplifying assumptions at the outset. We shall restrict ourselves entirely to the system of Ar adsorbed on Al, and consider mainly p-polarized light for which the electric field lies in the plane of incidence. Furthermore, we shall assume the polarizability of the adatom to be isotropic, i.e., $\overleftrightarrow{\alpha}(\omega)=\alpha(\omega)\overleftrightarrow{I}$, and given by the atomic value in free space. While this is indeed a limiting assumption, it is not possible as yet to compute the dynamical polarizability of an adatom very accurately.[10] We also feel that the effects we discuss in this paper will remain even if $\alpha(\omega)$ is changed; what will change are the location of absorption peaks and the magnitude of their shift caused by changing coverage. The manner in which we compute $\alpha(\omega)$ for Ar is described in some detail in Sec. II. Section III discusses the nonretarded screening model of I, and presents results on differential reflectance based on that model. In Sec. IV we present results of numerical calculations based on the SCIB model for the dynamical screening of oscillating dipoles. Section V summarizes our conclusions, and suggests ways of verifying the theoretical idea.

II. ADATOMIC POLARIZABILITY

We assume for the sake of simplicity that the polarizability of an adsorbed argon atom is isotropic and is given by the free-atom formula,[11,12]

$$\alpha(\omega)=\frac{e^2}{m}\sum_j \frac{f_j}{(\omega_j^2-\omega^2-i\gamma_j\omega)}, \tag{2.1}$$

in terms of the transition frequency ω_j and oscillator strength f_j for the jth transition. Here γ_j is a phenomenological damping term. No first-principles calculation exists for the dynamical polarizability of an argon atom adsorbed on the surface of a simple metal such as Al. In this calculation, therefore, we replace f_j and ω_j by their values in free space. This approximation, although drastic, is by no means an absurd one. Theoretical calculations[10] show that the static polarizabilities of noble-gas atoms brought near a jellium surface differ very little from their free-space values at separations $\gtrsim 2$ Å. Also differential reflectance data[2,3] at dilute coverage of adsorbates show optical-absorption peaks that lie close in energy to what is found in free atoms. However, the interpretation of the data is difficult, owing to large background signals. At optical frequencies we need to be concerned only with transitions of the six $3p$ electrons comprising the outer shell of argon. Expressing energy in eV, Eq. (2.1) may be rewritten as ($a_0=\hbar^2/me^2$, the Bohr radius),

$$\alpha(\omega)=6(27.2)^2a_0^3 \times\sum_\nu \frac{f_{3p\to\nu}}{E_{3p\to\nu}^2-(\hbar\omega)^2-i\hbar^2\gamma_\nu\omega}\,, \quad (2.22)$$

where $f_{3p\to\nu}$ refers to the oscillator strength of a *single* electron for transition to a final state labeled by ν with the associated transition energy $E_{3p\to\nu}$.

The sum in Eq. (2.2) consists of two parts: a discrete part for which $\nu=ns$ or nd, where n is the principal quantum number ≥ 3 and s and d refer to angular momentum values, and a continuum part where the transition energy exceeds the energy of ionization. For the discrete part of the sum we use the best theoretical and/or experimental values for the oscillator strengths and transition energies available in the literature.[13–15] These are tabulated in Table I for $3\leq n\leq 6$, which is the range of discrete transitions that we consider. For the continuum part of the sum, we approximate the curves for $df/d\epsilon$ given by Cooper[13] by piecewise linear functions suitably truncated so as to have the correct area under them as computed theoretically. Thus for $3p\to$ continuum d transitions, we assume

$$\frac{df}{d\epsilon}=\begin{cases}A-B\epsilon\,, & \epsilon\leq\epsilon_0\\ 0, & \epsilon>\epsilon_0\end{cases} \quad (2.3)$$

where ϵ is the kinetic energy of the excited electron,

$$A=1.6(\mathrm{Ry})^{-1}=0.1176(\mathrm{eV})^{-1}\,, \quad (2.4a)$$

$$B=1.45(\mathrm{Ry})^{-2}=0.0079(\mathrm{eV})^{-2}\,, \quad (2.4b)$$

and

$$\epsilon_0=1.1\ \mathrm{Ry}=14.96\ \mathrm{eV}\,. \quad (2.4c)$$

Clearly $h\omega=\epsilon+I$, where I is the ionization energy. For I we use the experimental value[14] of 15.76 eV. Cooper's calculated value[13] of 16.06 eV differs from it by only about 2%. For $3p\to$ continuum s transitions, we assume

$$\frac{df}{d\epsilon}=\begin{cases}0.80, & \epsilon\leq\tilde{\epsilon}_0\\ 0, & \epsilon>\tilde{\epsilon}_0\end{cases} \quad (2.5)$$

where $\tilde{\epsilon}_0=1$ Ry$=13.6$ eV. The approximations of Eqs. (2.4) and (2.5) yield

$$\sum_{\{E_s\}} f_{3p\to E_s}=0.08\,, \quad (2.6a)$$

$$\sum_{\{E_d\}} f_{3p\to E_d}=0.88\,, \quad (2.6b)$$

in agreement with Cooper's calculations.[13] Finally, in the continuum range of transitions, we set $\gamma_\nu=0^+$ and replace the sum over ν by appropriate integrals over ϵ. The integrals are easy to carry out and yield logarithmic functions.

The resulting electronic polarizability $\alpha(\omega)$ of argon is a function of the photon frequency ω, is complex, and depends on the choice of γ_ν for the discrete transitions. In many of the calculations reported below, we choose $\hbar\gamma_\nu=0.5$ eV for all ν to account for the substrate-induced broadening of the adsorbate energy levels in an approximate manner. All γ's of course need not be the same, and we shall discuss this point and its impact on our calculations later. At this stage we simply note that from Table I, the lowest excitation energy of a free argon atom comes from $3p\to 4s$ transition. The oscillator strength for that transition, however, is almost a factor of 4 smaller than that for the first allowed d transition ($3p\to 3d$). The basic assumption that we make in using the free-atom polarizability for the adsorbed argon atom is

TABLE I. Table of values of transition energies and oscillator strengths of argon atom used in these calculations.

ν	$E_{3p\to\nu}$ (eV)	$f_{3p\to\nu}$
$4s$	11.57	0.055
$5s$	14.33	0.0082
$6s$	14.96	0.0031
$3d$	14.076	0.196
$4d$	14.89	0.081
$5d$	15.29	0.043
$6d$	15.48	0.022

that the above mentioned features survive, at least approximately, even after the atom is adsorbed. The assumption appears to be justified experimentally,[3] where differential reflectance for dilute coverage of Ar on Al shows peaks whose positions correlate well with the optical-absorption peaks in the free atom. This is especially true of the $3p \rightarrow 4s$ transtion. The $3p \rightarrow 3d$ transition, however, is masked by a rising background. How the oscillator strengths are affected by adsorption is much less clear. Since an argon atom chemisorbs weakly on a metal surface, we do not expect its $3p$, and possibly $3d$, states to be modified greatly by adsorption. The excited $4s$ state, though, is clearly alkalilike[3] and would be perturbed by the metal. Nevertheless, we feel that the experimental data justify, albeit qualitatively, our procedure of using the free-space polarizability to describe the response of the adsorbed argon atom.

III. THE IMAGE RESPONSE

Let us imagine that argon atoms are adsorbed on the surface of Al in an ordered two-dimensional array. The experiments that we shall focus on here were carried out on substrates of polycrystalline Al, and the structure of adsorbed overlayers of Ar on the them is not known. We assume the overlayer geometry to be square for simplicity; that suffices for our purpose here since the present study of the local-field effect is aimed primarily at a qualitative, physical understanding of it rather than at quantitative answers. Let the square array have a lattice parameter a_l, the atomic locations being given by $\vec{R}_{ij}$ of Eq. (1.1). As discussed in Sec. I, long-wavelength electromagnetic waves incident on the system will induce in each adatom a dipole moment $\vec{p}$ which depends on both the external and dipolar electric fields. The dipolar field [cf. Eq. (1.3)] consists of two parts, a part $\vec{E}^{(1)}_{\rm dip}$ arising from dipoles lying in the adsorbate plane, and a part $\vec{E}^{(2)}_{\rm dip}$ coming from dynamical screening of the metal. It is straightforward to calculate $\vec{E}^{(1)}_{\rm dip}$, and the result is given in Eqs. (1.5). It is much harder to deal with the dynamical screening of the metal, and some form of approximation must be introduced. In this and the following section, we examine some of these approximations.

It was assumed in I that the dynamical screening of an oscillating point dipole by a metal surface could be described by the classical theory of images.[16] This section will be devoted to studying the consequences of that assumption. The next section will be devoted to the question of nonlocal corrections. According to the classical image theory, a dipole $\vec{p}$ located at $\vec{R}_{ij}=(ia_l,ja_l,-z_0)$ in front of a metal surface will induce an image dipole

$$\vec{p}_I=\frac{(\epsilon-1)}{(\epsilon+1)}(-p_x,-p_y,p_z) \tag{3.1}$$

located at

$$\vec{R}^{\,I}_{ij}=(ia_l,ja_l,z_0)\ , \tag{3.2}$$

where i and j are integers lying between $-\infty$ and $+\infty$, and $\epsilon=\epsilon(\omega)$ is the frequency-dependent, complex dielectric constant of the metal. The image theory is, in fact, valid in the nonretarded limit, so that in applying it to the present situation, we would ignore all retardation effects. The induced dipolar field $\vec{E}^{(2)}_{\rm dip}$ at the adatom site specified by $(0,0,-z_0)$ is now given by a sum similar to that in Eq. (1.4) with $\vec{p}_I$ replacing $\vec{p}$, $\vec{R}^{\,I}_{ij}$ replacing $\vec{R}_{ij}$, and the term $i=j=0$ now included in the sum to account for the effect at a dipolar site of its own image. The Cartesian components of the induced dipolar field are given by

$$[\vec{E}^{(2)}_{\rm dip}]_i=(p_i/a_l^3)\xi_I/2,\quad i=x,y \tag{3.3}$$

$$[\vec{E}^{(2)}_{\rm dip}]_z=(p_z/a_l^3)\xi_I\ , \tag{3.4}$$

where

$$\xi_I=\frac{(\epsilon-1)}{(\epsilon+1)}\sum_{i,j=-\infty}^{\infty}\frac{3(2z_0/a_l)^2-[i^2+j^2+(2z_0/a_l)^2]}{[i^2+j^2+(2z_0/a_l)^2]^{5/2}}\ . \tag{3.5}$$

A large body of literature[17,18] exists on dipolar sums of this type. The particular two-dimensional lattice sum of interest here was carried out by Mahan and Lucas.[19] The sum can be converted into a more rapidly convergent series:

$$\xi_I=\frac{(\epsilon-1)}{(\epsilon+1)}16\pi^2\sum_{i=0}^{\infty}\sum_{j=1}^{\infty}(i^2+j^2)^{1/2}\exp[-(4\pi z_0/a_l)(i^2+j^2)^{1/2}]\ . \tag{3.6}$$

Combining Eqs. (3.3) and (3.4) with Eqs. (1.2)–(1.5), we can express the induced dipole moment on an adatom as a function of the external electric field $\vec{E}^{\,0}$. It is convenient to introduce a length parameter d, which denotes the equivalent thickness of the adsorbate layer, such that the

volume per adatom is $a_l^2 d$. We say nothing physically about the size of d since the final results are independent of it. Let us define

$$\Gamma(\omega)=\alpha(\omega)/a_l^3 , \tag{3.7a}$$

$$\vec{P}=\vec{p}/(a_l^2 d) , \tag{3.7b}$$

the latter being the dipole moment per unit volume in the adsorbate layer. Then, after a modest amount of algebra, we obtain

$$P_i=(\Gamma a_l/d)E_i^0/[1+(\Gamma/2)(\xi_0-\xi_I)] , \quad i=x,y \tag{3.8}$$

and

$$P_z=(\Gamma a_l/d)E_i^0/[1-\Gamma(\xi_0+\xi_I)] . \tag{3.9}$$

The frequency dependence of Γ is suppressed in these equations along with that of ξ_I (through ϵ). It will be displayed explicitly whenever it is necessary to do so.

We now use Eqs. (3.8) and (3.9) to define the macroscopic electric field in the adsorbed layer, and hence its effective dielectric constant. Using the continuity of the normal component of the displacement field and the tangential component of the electric field, which allows us to identify E_x^0, E_y^0, and E_z^0 with the macroscopic fields E_x, E_y, and D_z in the film, we have

$$E_i^0+4\pi P_i=\epsilon_i E_i^0, \quad i=x,y \tag{3.10}$$

$$E_z^0-4\pi P_z=\epsilon_z^{-1}E_z^0 . \tag{3.11}$$

As a result, we find that the adsorbate film may be characterized by an anisotropic dielectric tensor whose components satisfy the relations

$$\epsilon_i-1=4\pi\Gamma(a_l/d)/[1+(\Gamma/2)(\xi_0-\xi_1)] , \quad i=x,y \tag{3.12}$$

$$\epsilon_z^{-1}-1=-4\pi\Gamma(a_l/d)[1-\Gamma(\xi_0+\xi_1)] . \tag{3.13}$$

These dielectric response functions are all that are needed to compute the differential reflectance of light from an adsorbate-covered metal surface.[4] The results, for s- and p-polarized light, respectively, are given by

$$\left[\frac{\Delta R_s}{R_s}\right]=4\left[\frac{\omega}{c}\right]d\cos\theta_i \ \mathrm{Im}\left[\frac{\epsilon_y-1}{\epsilon-1}\right] , \tag{3.14}$$

$$\left[\frac{\Delta R_p}{R_p}\right]=4\left[\frac{\omega}{c}\right]d\cos\theta_i \ \mathrm{Im}\left[\frac{(\epsilon-\sin^2\theta_i)(\epsilon_x-1)+\epsilon^2\sin^2\theta_i(\epsilon_z^{-1}-1)}{(1-\epsilon)(\sin^2\theta_i-\epsilon\cos^2\theta_i)}\right] . \tag{3.15}$$

Here θ_i is the angle of incidence of light. As mentioned earlier, the differential reflectance is independent of the thickness d of the adsorbate layer since both (ϵ_i-1) and $(\epsilon_z^{-1}-1)$ are inversely proportional to d.

Figure 1 shows the differential reflectance per unit coverage, i.e., $(\Delta R_p/R_p)/\Theta$ with Θ being the coverage for p-polarized light incident on argon-covered Al at two values of the converage, viz., $\Theta=25\%$ and 100%. The adsorbate geometry on the metal surface is always assumed to be given by a square lattice; only the lattice parameter a_l doubles in magnitude on going from full to quarter coverage. The angle of incidence is taken to be 45°. The input parameters in the calculation, apart from the dimensionless polarizability $\Gamma(\omega)$, are the lattice parameter a_l, and the distance z_0 from the surface, and the complex dielectric constant $\epsilon(\omega)$ of the substrate metal. We choose $a_l=4$ and 8 Å for full and quarter coverage. The former value corresponds approximately to a monolayer coverage as suggested by experiments on the physisorp-

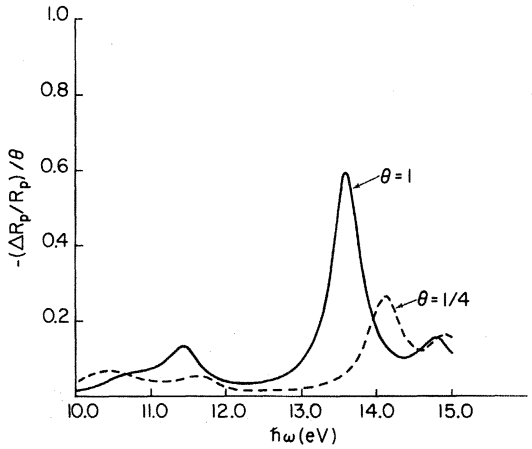

FIG. 1. Calculated differential reflectance per unit coverage of p-polarized light from the system of argon-covered aluminum at two coverages. Solid line refers to a full monolayer and dashed line to a quarter monolayer. The calculations are based on a local model for the substrate dielectric response. All discrete transitions on the adatom have been assumed to have the same energy width of 0.5 eV.

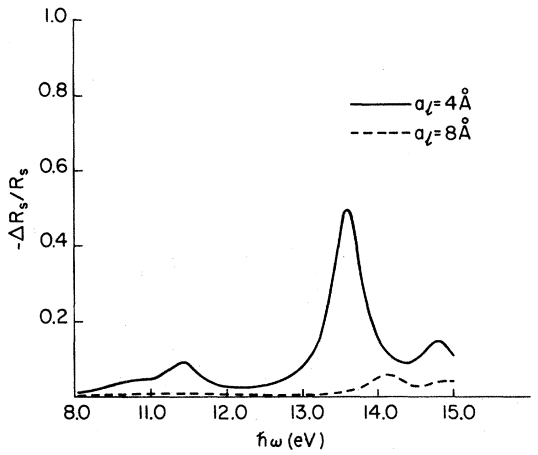

FIG. 2. Calculated differential reflectance of *s*-polarized light from the system of argon-covered aluminum at two coverages. Solid line refers to a full monolayer and dashed line to a quarter monolayer. The calculations are based on a local model for the substrate dielectric response. All discrete transitions on the adatom have been assumed to have the same energy width of 0.5 eV.

tion of argon on graphite.[20] We take $z_0=2$ Å in these calculations. The dielectric constant of aluminum is taken from a Kramers-Kronig analysis[21] of the experimental reflectance data. Figure 2 shows similar results for the differential reflectance of *s*-polarized light for two coverages of argon on aluminum. Note that the differential reflectance of Fig. 2 has not been normalized to unit coverage. The results of the two figures are very similar, indicating that the prominent peaks arise from structures in $\mathrm{Im}(\epsilon_x-1)$. Our finding is confirmed by the recent experimental data.[22] Model calculations[23] show that additional structures in the differential reflectance of *p*-polarized light, coming from the term involving $(\epsilon_z^{-1}-1)$ in Eq. (3.15), are important near the longitudinal normal mode of the adlayer. The frequency range displayed in Fig. 1 presumably does not lie close to that normal mode.

The most interesting feature of the results shown in Figs. 1 and 2 is that they do not scale simply with coverage. Rather we notice a characteristic movement of the differential reflectance peaks as a function of photon frequency as the coverage is changed, and this movement is fairly insensitive to the polarization of light. These features arise from the fact that the adsorbed atoms, in our theory, are not regarded simply as independent scatterers. Their interaction—the so-called "local-field effect"—is explicitly included in our calculation. The change of peak location with coverage is an important manifestation of the local-field effect, and its presence is indeed confirmed by recent experiments.[2,3,22] The local-field effect is also the reason why the magnitudes of differential reflectance peaks are not simply proportional to the coverage.

Recent experimental data of Cunningham, Greenlaw, and Flynn[22] on the system of argon-covered aluminum unmistakably reveal the presence of adsorbate-adsorbate interaction in the differential reflectance spectra. The main findings of these authors may be summarized as follows. At coverages above a monolayer, they find a peak at around 11.7 eV, a weak peak or shoulder at around 13 eV, and a steadily rising shoulder culminating in a peak in the (16—17)-eV range. The high-energy peak, occurring above the plasma energy, is beyond the scope of the local theory discussed in this section. The low-energy peak is atomiclike and shows effects of spin-orbit splitting at coverages in excess of two monolayers. As the coverage is decreased to $\Theta=25\%$, the low-energy peak remains fairly stationary but broadens somewhat and weakens in strength. The shoulder or weak peak at 13 eV, on the other hand, has an unmistakable shift to higher energies as the coverage of argon is reduced. These results, in broad terms, are true for both polarizations although the structures differ somewhat in detail.

The classical calculations reported here lead to a qualitative understanding of these structures in the differential reflectance data. A detailed comparison of the theory with the experiment would, of course, be premature. Nevertheless, we can identify the low-energy peak with the $3p\rightarrow 4s$ transition and the second peak with the $3p\rightarrow 3d$ transition on the adsorbed atom. While the $3p\rightarrow 4s$ transition energy on the adsorbate has roughly the atomic value, the $3p\rightarrow 3d$ transition energy is lower than the atomic value by more than a volt at a monolayer coverage. Part of the shift, as shown in Fig. 1, may be explained by the local-field effect associated with a transition having a rather large oscillator strength. The rest must be attributed to chemical shift or adsorbate-substrate interaction. Similarly, the relatively rapid movement of the higher-energy peak as a function of the adsorbate coverage, as compared to the slower movement of the lower-energy peak, can be understood in terms of differences in oscillator strengths.

Comparison of the experimental data with the calculations reported in Figs. 1 and 2, however, re-

veals two glaring deficiencies. The major one concerns the relative peak heights, where experimentally the $3p \rightarrow 4s$ transition peak is stronger than the $3p \rightarrow 3d$ transition peak, in contradistinction to the result shown in Fig. 1. A second difficulty is that the lower-energy peak in Fig.1 shows a slightly greater movement as a function of coverage than is seen experimentally. Furthermore, the calculated differential reflectance is substantially larger in magnitude than what is observed in experiments. In the next section we shall discuss how nonlocal corrections might modify our results. However, we wish to note here one possible way of interpreting the experimental observation within the present context. In calculating $\alpha(\omega)$ and hence $\Gamma(\omega)$, we assumed $\hbar\gamma_\nu = 0.5$ eV for all ν [cf. Eq. (2.2)]. This implies that all atomic levels broaden approximatley equally upon adsorption, an assumption that is far too restrictive. Instead it makes sense to assume that the higher-energy atomic levels have more broadening when the atom comes close to the metal surface. We have explored theoretically the consequences of the choice $\hbar\gamma_\nu = 0.5$ eV for the $3p \rightarrow 4s$ transition and a series of values of $\hbar\gamma_\nu$ ($=1.0$, 1.5, and 2.5 eV) for all the other transitions. We find that the higher-energy peak in differential reflectance broadens and decreases in strength as a result of that assumption. The effect can be seen quite clearly in Fig. 3 where we have plotted the normalized differential reflectance for p-polarized light under the assumption that $\hbar\gamma_\nu = 2.5$ eV for all transitions with energies above the including the $3p \rightarrow 3d$ transition. The lower-energy peak is now seen to be the stronger one.

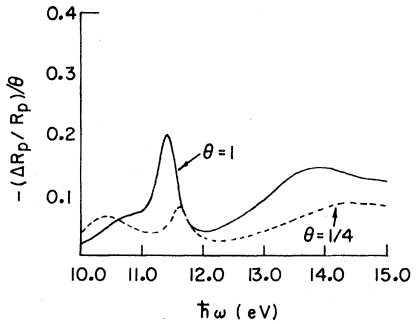

FIG. 3. Calculated differental reflectance per unit coverage of p-polarized light from the system of argon-covered aluminum at two coverages. Solid line refers to a full monolayer and dashed line to a quarter monolayer. A local dielectric function has been used in these calculations to describe the substrate response. Discrete transitions on the adatom are presumed to have the same energy width of 2.5 eV except for the lowest transition ($3p \rightarrow 4s$) which has the energy width of 0.5 eV.

The higher-energy peak has broadened considerably and moves much more slowly with coverage. This behavior agrees qualitatively with the experimental observation.[22] The magnitude of differential reflectance in Fig. 3 is also closer to the experimental data. It would certainly have been possible to obtain closer agreement between the calculated and experimental differential reflectance by treating $\hbar\gamma_\nu$ as adjustable parameters. Such an approach, however, is not very worthwhile, given the unsophisticated nature of the theoretical calculation. In fact, nonlocal calculations reported in the next section do not include studies of the sensitivity of the results on varying $\hbar\gamma_\nu$, although the effect is expected to be similar to that shown in Fig. 3.

IV. EFFECT OF NONLOCAL RESPONSE OF THE SUBSTRATE

In the preceding section the dielectric response of the substrate was described by a local function. In this section we wish to study the consequences of including the nonlocality of the substrate response function in our calculation. Specifically we wish to calculate the image potential due to an ordered monolayer of dipoles situated on top of a nonlocal substrate. The response of the latter will be described by the specular-scattering or semiclassical infinite barrier (SCIB) model, which has been discussed widely in the literature.[24,25] Although this model does not treat the diffuse nature of the metal surface correctly, it includes the most important effects of nonlocality. It can be solved easily for arbitrary distance of the dipole from the surface and for different metals, and the results are expected to be valid when the dipole separation from the surface, z_0, is $\gtrsim 2$ Å.

Let us consider first a single, oscillating point dipole, $\vec{p}(t) = \vec{p}e^{-i\omega t}$, located at $\vec{r}_j = (\vec{\rho}_j, -z_0)$ in front of a metal surface, where the metal is imagined to fill the half-space $z > 0$. The distance z_0 between the dipole and the metal surface is restricted to be much smaller than the wavelength of light, so retardation can be neglected. Then, as shown by Fuchs and Barrera,[9] the induced potential can be written as (suppressing the time-dependent factor)

$$\Phi'(\vec{r};\vec{r}_j) = \int \frac{d^2q_1}{(2\pi)^2} \Phi'(\vec{q}_i, z; \vec{r}_j) e^{i\vec{q}_1 \cdot \vec{\rho}} , \quad (4.1)$$

where

$$\Phi'(\vec{q}_1, z; \vec{r}_j) = 2\pi p_z B(q_1) e^{q_1(z-z_0)} e^{-i\vec{q}_1 \cdot \vec{\rho}_j} \quad (4.2)$$

when the dipole moment lies in the z direction. Here the function $B(q_1)$ is defined as

$$B(q_1)=[I(q_1)-1][I(q_1)+1] \tag{4.3}$$

for a two-dimensional wave vector $\vec{q}_1$ in the xy plane, and

$$I(q_i)=\frac{q_1}{\pi}\int_{-\infty}^{\infty}\frac{dq_z}{q^2\epsilon_l(\vec{q},\omega)}\ , \tag{4.4}$$

where $\epsilon_l(\vec{q},\omega)$ is the frequency- and wave-vector-dependent bulk longitudinal dielectric constant of the metal and $q^2=q_1^2+q_z^2$. Similarly, for a dipole lying in the x direction, the induced potential is given by the same expression as Eq. (4.1), except that the Fourier transform is now given by

$$\Phi'(\vec{q}_1,z,\vec{r}_j)=-2\pi p_x\frac{iq_{1x}}{q_1}B(q_1) \times e^{q_1(z-z_0)}e^{-i\vec{q}_1\cdot\vec{\rho}_j}\ . \tag{4.5}$$

Next consider an ordered, square array of dipoles situated on the plane $z=-z_0$. Let a_l be the lattice parameter. The induced potential at a given point is now obtained simply by superposition. Thus, for all dipoles pointing in the z direction, the net induced potential has the Fourier transform

$$\Phi'_{\rm tot}(\vec{q}_1,z)=2\pi p_z B(q_1)e^{q_1(z-z_0)} \times\sum_{\{\vec{\rho}_j\}}e^{-i\vec{q}_1\cdot\vec{\rho}_j}\ . \tag{4.6}$$

Substitution in Eq. (4.1) leads to the net induced potential in space,

$$\Phi'_{\rm tot}(\vec{r})=\frac{2\pi p_z}{a_l^2}\sum_{\{\vec{G}\}}B(G)e^{G(z-z_0)}e^{i\vec{G}\cdot\vec{\rho}}\ , \tag{4.7}$$

where $\{\vec{G}\}$ denotes the set of two-dimensional reciprocal-lattice vectors corresponding to the adsorbate lattice. Similarly, for all dipoles pointing in the x direction, the net induced potential in space is

$$\Phi'_{\rm tot}(\vec{r})=\frac{2\pi p_x}{a_l^2}\sum_{\{\vec{G}\}}\frac{-iG_x}{G}B(G)e^{G(z-z_0)}e^{i\vec{G}\cdot\vec{\rho}}\ . \tag{4.8}$$

The induced electric field is readily calculated from Eqs. (4.7) and (4.8). At a dipolar site specified by $(0,0,-z_0)$ the induced field has components

$$E_z^{\rm ind}(0,0-z_0)=-\frac{2\pi}{a_l^2}p_z\sum_{\{\vec{G}\}}B(G)Ge^{-2Gz_0} \tag{4.9}$$

and

$$E_x^{\rm ind}(0,0,-z_0)=-\frac{2\pi}{a_l^2}p_x\tfrac{1}{2}\sum_{\{G\}}B(G)Ge^{-2Gz_0}\ . \tag{4.10}$$

In deriving Eq. (4.10) we used the rotational symmetry property of the square lattice, so that the lattice sum of G_x^2/G^2 ultimately contributes only a factor of $\frac{1}{2}$. Also in the sums over $\{\vec{G}\}$, terms involving an odd power of G_x vanish owing to reflection symmetry. Thus the net induced field in the z direction depends only on the z component of the dipole moment, and the same is true of the field in the x direction. Equations (4.9) and (4.10) are, therefore, valid for arbitrary orientation of the dipole moment $\vec{p}$.

It is useful to point out that the nonlocality of the dielectric response of the metal substrate and the associated spatial dispersion enter our problem through the functions $I(q_1)$ and $B(q_1)$. The spatial dispersion has important physical effects including the broadening of the surface-plasmon resonance. For a local substrate, $\epsilon_l(\vec{q},\omega)\to\epsilon(\omega)$, and Eq. (4.4) is readily integrated to yield

$$I(q_1)\underset{\text{local limit}}{\longrightarrow}1/\epsilon(\omega)\ , \tag{4.11}$$

$$B(q_1)\underset{\text{local limit}}{\longrightarrow}-[\epsilon(\omega)-1]/[\epsilon(\omega)+1]\ . \tag{4.12}$$

It is now a relatively straightforward matter to recover the results of Sec. III from those of this section.

We proceed with our present analysis by considering the adsorbate array in detail. For a square lattice the reciprocal-lattice vectors are given by

$$\vec{G}=\frac{2\pi}{a_l}(i\hat{x}+j\hat{y})\ , \tag{4.13}$$

where i and j are integers which may be positive, negative, or zero. We substitute this in Eqs. (4.9) and (4.10) and use the notation of Sec. I. The net dipolar field $\vec{E}_{\rm dip}$ at the site of an adsorbed atom now has components

$$[\vec{E}_{\rm dip}]_z=\frac{P_z}{a_l^3}(\xi_0+\xi_I)\ , \tag{4.14}$$

$$[\vec{E}_{\rm dip}]_x=\tfrac{1}{2}\frac{p_x}{a_l^3}(-\xi_0+\xi_I)\ , \tag{4.15}$$

where

$$\xi_0 = -9.0336 \tag{4.16a}$$

and

$$\xi_I = -(2\pi)^2 \sum_{i,j=-\infty}^{\infty} B(i,j)(i^2+j^2)^{1/2} \times \exp[-(4\pi z_0/a_l) \times (i^2+j^2)^{1/2}] . \tag{4.16b}$$

Here $B(i,j)=B(G)$ with

$$G=(2\pi/a_l)(i^2+j^2)^{1/2} .$$

These formulas are structurally similar to those derived in the preceding section for a local substrate. In fact, the use of Eq. (4.12) along with a simple rearrangement of terms allows us to identify Eq. (4.16b) exactly with Eq. (3.6). The rest of the logic of Sec. III now applies naturally to the analysis of this section. From the self-consistency condition of Eq. (1.2) for the induced dipole moment, and the defining relations embodied in Eqs. (3.10) and (3.11), we can define the "effective" bulk dielectric response tensor of the adsorbate layer. Thus Eqs. (3.14) and (3.15) are still valid for differential reflectance. The only effect of nonlocality is to change the definition of ξ_I, the response of the metal to an ordered dipole layer. For a local substrate $B(i,j)$ is a constant, i.e., all reciprocal-lattice vectors contribute equally to $B(G)$. This is no longer true when nonlocality of the substrate response is taken into account.

To assess the importance of the nonlocal correction, we have calculated $B(i,j)$ within the hydrodynamic model for the bulk dielectric constant of the metal. The metal is now described by the response function[9]

$$\epsilon_l(\vec{q},\omega)=1-\frac{\omega_p^2}{\tilde{\omega}^2-\beta^2 q^2} , \tag{4.17}$$

where $\tilde{\omega}^2=\omega(\omega+i/\tau)$, τ being a phenomenological relaxation time, ω_p is the plasma frequency, $\beta^2=(\frac{3}{5})v_F^2$, and $q^2=q_1^2+q_z^2$. Although this dielectric constant becomes invalid at low frequencies and does not contain electron–hole-pair excitations, it gives a qualitatively correct description of the bulk-plasmon and surface-plasmon dispersion. With the use of this dielectric function, Eq. (4.4) may be evaluated analytically to yield [cf. Eqs. (47) and (48) of Ref. 9]

$$I(q_1)=1+\frac{\omega_p^2}{\tilde{\omega}^2-\omega_p^2}\left[1-\frac{q_1}{\tilde{\Gamma}}\right] , \tag{4.18}$$

where

$$\tilde{\Gamma}(q_1)=\left[q_1^2+\frac{\omega_p^2-\tilde{\omega}^2}{\beta^2}\right]^{1/2} . \tag{4.19}$$

Note that $\tilde{\Gamma}$ is complex and depends on both wave vector and frequency. Substituting Eq. (4.18) into Eqs. (4.3) and (4.16b) with $q_1=G$, we obtain

$$\xi_I = -(2\pi)^2 \sum_{i,j=-\infty}^{\infty} \frac{[(i^2+j^2)^{1/2}-\tilde{\Gamma}(i,j)](i^2+j^2)^{1/2}}{(i^2+j^2)^{1/2}+\left[\frac{\epsilon_{\rm loc}+1}{\epsilon_{\rm loc}-1}\right]\tilde{\Gamma}(i,j)} e^{-4\pi(i^2+j^2)^{1/2}z_0/a_l} , \tag{4.20}$$

where

$$\epsilon_{\rm loc}=1-\omega_p^2/\tilde{\omega}^2 \tag{4.21}$$

is the effective, local dielectric function, and

$$\tilde{\Gamma}(i,j)=(a_l/2\pi)\tilde{\Gamma}(G) \tag{4.22}$$

is the dimensionless form of $\tilde{\Gamma}(q_1)$ with

$$q_1=G=\frac{2\pi}{a_l}(i^2+j^2)^{1/2} .$$

The local limit is recovered on letting $\beta\to 0$; then $\tilde{\Gamma}(i,j)\to\infty$ and Eq. (4.20) reduces to Eq. (3.6).

We have computed the differential reflectance of Eq. (3.15) in this nonlocal case, when ξ_I is given by the expression (4.20). The results for Ar on Al are shown in Fig. 4 for the normalized differential reflectance of p-polarized light at two coverages, viz., $\Theta=\frac{1}{4}$ and 1. The results for the nonlocal case are shown by the solid lines, while the dashed lines represent the corresponding local situation, and are displayed for comparison purposes. For the best "hydrodynamic" dielectric constant of aluminum, we chose $(\omega_P\tau)^{-1}=0.0532$ since it gave the best fit to the experimental data in the (10–15)-eV range,[21] and β was evaluated from the known Fermi momentum of the metal. The corresponding local situation is described by the Drude formula on setting $\beta=0$. The polarizability of Ar was calculated in the manner described in Sec. II with $\hbar\gamma_\nu=0.5$ eV for all discrete transitions.

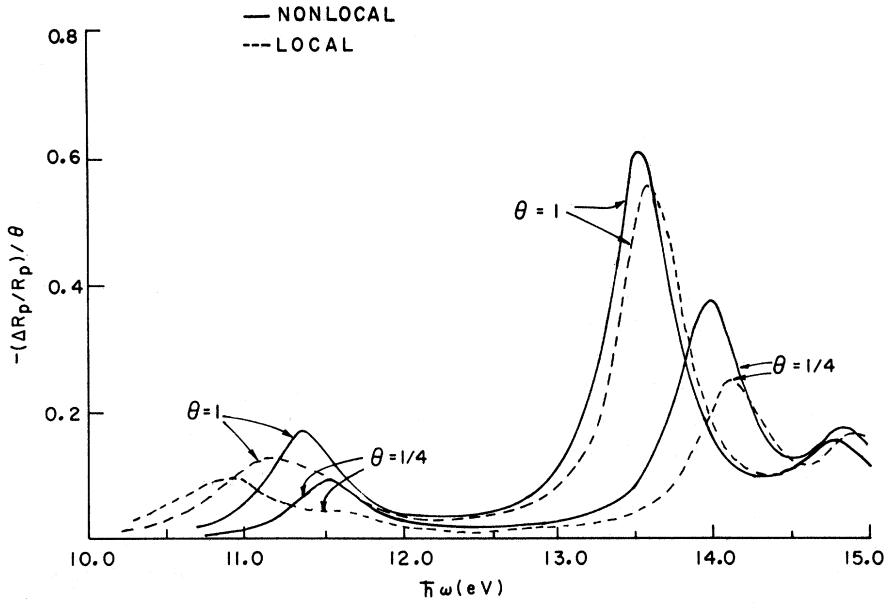

FIG. 4. Comparison of local (dashed lines) and nonlocal or SCIB (solid lines) models for the substrate response function with regard to their effect on the normalized differential reflectance of p-polarized light from the system of argon-covered aluminum. Calculated results are presented for two values of the coverage Θ. All discrete transitions on the adatom are presumed to have the same energy width of 0.5 eV.

One thing is quite clear from the curves of Fig. 4. The local-field effect, as exemplified by the movement of differential reflectance peaks upon changing the adsorbate coverage, certainly is present even after including the nonlocality of the substrate dielectric response. We conclude that the local-field effect seen in differential reflectance is physically fundamental in origin, and it is unaffected by the detailed nature of the substrate response function. There are, however, certain characteristic differences between the local and unlocal cases as revealed by the curves of Fig. 4. For example, the effect of nonlocality appears to be more important at lower coverages than at higher coverages. Also nonlocality apparently enhances the magnitude of differential reflectance. These features perhaps can be correlated with the fact that a large number of terms contributes to the sum in Eqs. (4.16b) or (4.20) at lower coverages when a_l is relatively large, but we have not explored this point in any depth. A second interesting difference between the local and nonlocal situations is evident in the (10—12)-eV energy region. There, the local case shows two peaks that arise from an interaction between the $3p \rightarrow 4s$ atomic transition and the surface-plasmon resonance (related to the presence of the quantity $[\epsilon(\omega)+1]$ in the denominator of Eq. (3.6)). In the nonlocal theory, however, the surface-plasmon resonance is broadened and there is no splitting of the atomic transition.[9] Finally we note that the movement or shift of peaks as a function of coverage is somewhat reduced in the nonlocal case. None of these features, though, detract from the fact that the local-field effect is important in differential reflectance from adsorbed overlayers, and it must be included in a serious calculation.

V. CONCLUSIONS

In this paper we have amplified on the work of Ref. 1 and studied the role of the local-field effect in differential reflectance from an adsorbed overlayer on a metal surface. We describe the dynamical screening of the adsorbate dipoles (induced by the electromagnetic field) by the metal substrate two different models of its dielectric response, viz., a local dielectric function, and a nonlocal response based on the SCIB model. In both cases, we find the local-field effect to be quite important, and it is essential for interpretating the coverage dependence of differential reflectance. Model theoretical calculations have been done for the system of argon adsorbed on aluminum, and experimental data on the same system are in broad agreement with the results of the calculations. Admittedly the

theoretical calculations are based on a number of simplifying assumptions that make them only qualitatively valid. For example, the polarizability of an adsorbed argon atom is assumed to be given by the atomic polarizability in free space. Also the adsorbate geometry is assumed to be a square, although no structural information is available about the actual experimental system. Neither assumption has a critical influence on the physics of the problem. They affect only the details of the numerical results, e.g., the actual position of optical-absorption peaks and the magnitude of their movement as a function of adsorbate coverage. The experiments that we study here[22] were carried out at low enough temperatures that the adsorbed atoms would be immobile on the surface. Their actual geometrical configuration (e.g., triangular instead of square) will undoubteldy affect $\vec{E}^{(1)}_{dip}$, the dipolar field at an adatom due to all other atoms in the adsorbate plane, by changing the numerical value of ξ_0 of Eq. (1.5). But that will not alter the basic conclusions reached in this paper about the importance of the local-field effect in differential reflectance spectroscopy.

The fact that we have demonstrated in this paper the importance of the local-field effect within two quite different models of the substrate response function means that the effect is fundamental. It is present even when other forms[7] are used for the nonlocal dielectric constant of the substrate. We believe that the most important contribution to the dipolar field at an adsorbed atom comes from the neighboring atoms in the adsorbed layer, at least in the frequency range explored in our work. Experimental data on other adsorbate-substrate combinations with better characterized surface structure and adsorbate geometry would be essential for verifying beyond any doubt the conclusions derived in this paper.

ACKNOWLEDGMENTS

One of the authors (R.G.B.) is grateful to Luis Mochán for many helpful discussions and wishes to thank the Ames Laboratory for financial assistance. The Ames Laboratory is operated by the U. S. Department of Energy under Contract No. W-7405-Eng-82. This work was supported in part by the Director for Energy Research Office of Basic Energy Sciences.

[1]A. Bagchi, R. G. Barrera, and B. B. Dasgupta, Phys. Rev. Lett. 44, 1475 (1980).
[2]J. E. Cunningham, D. Greenlaw, J. L. Erskine, R. P. Layton, and C. P. Flynn, J. Phys. F 7, L281 (1977).
[3]J. E. Cunningham, D. Greenlaw, C. P. Flynn, and J. L. Erskine, Phys. Rev. Lett. 42, 328 (1979).
[4]A. Bagchi, R. G. Barrera, and A. K. Rajagopal, Phys. Rev. B 20, 4824 (1979).
[5]See, e.g., J. D. Jackson, *Classical Electrodynamics* (Wiley, New York, 1962), Chap. 4.
[6]J. Topping, Proc. Soc. (London) Ser. A 114, 67 (1927).
[7]P. J. Feibelman, Phys. Rev. B 22, 3654 (1980).
[8]T. Maniv and H. Metiu, Phys. Rev. B 22, 4731 (1980).
[9]R. Fuchs and R. G. Barrera, Phys. Rev. B 24, 2940 (1981); W. H. Weber and G. W. Ford, Phys. Rev. Lett. 44, 1774 (1980).
[10]The static polarizability of an atom adsorbed on the surface of jellium has been considered in C. Meixner and P. R. Antoniewicz, Phys. Rev. B 13, 3276 (1976).
[11]U. Fano and J. W. Cooper, Rev. Mod. Phys. 40, 441 (1968).
[12]J. M. Ziman, *Principles of the Theory of Solids* (Cambridge University Press, Cambridge, 1965), Chap. 8.
[13]J. W. Cooper, Phys. Rev. 128, 681 (1962).
[14]*Argon, Helium and the Rare Gases,* edited by G. A. Cook (Interscience, New York, 1961), p. 99.
[15]Y. A. Fugol, Adv. in Phys. 27, 1 (1978).
[16]J. D. Jackson, *Classical Electrodynamics* (Wiley, New York, 1962), Chap. 4.
[17]B. M. E. Van der Hoff and G. C. Benson, Can. J. Phys. 31, 1087 (1953).
[18]B. R. A. Nijboer and F. W. deWette, Physica (Utrecht) 23, 309 (1957); 24, 422 (1958).
[19]G. D. Mahan and A. A. Lucas, J. Chem. Phys. 68, 1344 (1978).
[20]C. G. Shaw, S. C. Fain, Jr., and M. D. Chinn, Phys. Rev. Lett. 41, 955 (1978).
[21]H. Ehrenreich, H. R. Philipp, and B. Segall, Phys. Rev. 132, 1918 (1963).
[22]J. A. Cunningham, D. K. Greenlaw, and C. P. Flynn, Phys. Rev. B 22, 717 (1980).
[23]M. H. Lee and A. Bagchi, Phys. Rev. B 22, 1687 (1980).
[24]R. Fuchs and K. L. Kliewer, Phys. Rev. 185, 905 (1969).
[25]G. Mukhopadhyay and S. Lundqvist, Phys. Scr. 17, 69 (1978).